Published in Chemistry A European Journal (Chem. Eur. J., 2021, 27, 7489-7501), which should be cited to refer to this work

Semiconductors |*Reviews Showcase*|

The Prospect of Dimensionality in Porous Semiconductors

Patrick W. Fritz and Ali Coskun*[a]

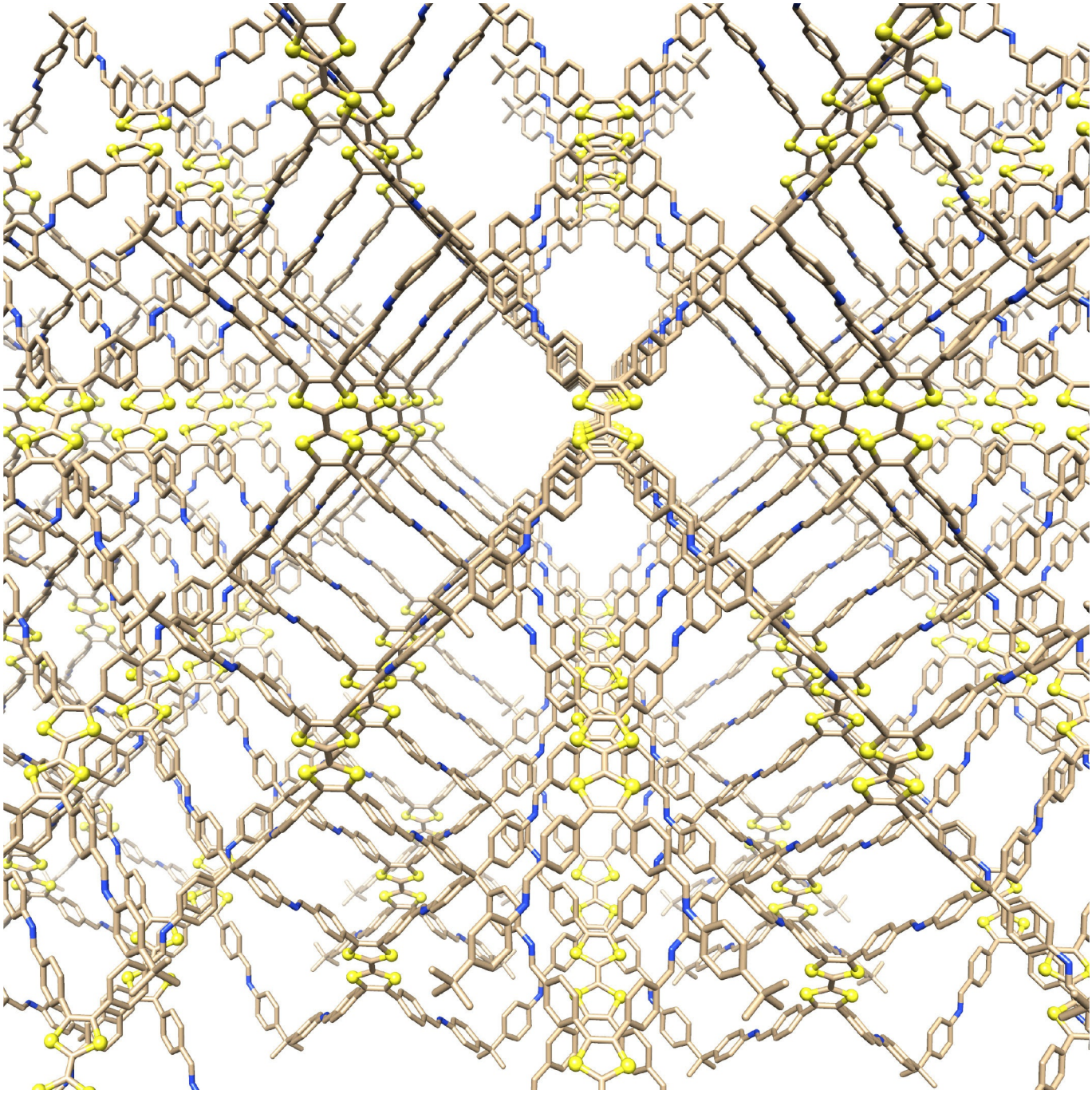

Abstract: With the advent of silicon-based semiconductors, a plethora of previously unknown technologies became possible. The development of lightweight low-dimensional organic semiconductors followed soon after. However, the efficient charge/electron transfers enabled by the non-porous 3D structure of silicon is rather challenging to be realized by their (metal-)organic counterparts. Nevertheless, the demand for lighter, more efficient semiconductors is steadily increasing resulting in a growing interest in (metal-)organic semiconductors. These novel materials are faced with a variety of challenges originating from their chemical design, their packing and crystallinity. Although the effect of molecular design is quite well understood, the influence of dimensionality and the associated change in properties (porosity, packing, conjugation) is still an uncharted area in (metal-)organic semiconductors, yet highly important for their practical utilization. In this Minireview, an overview on the design and synthesis of porous semiconductors, with a particular emphasis on organic semiconductors, is presented and the influence of dimensionality is discussed.

1. Introduction

Organic and metal–organic semiconductors have been a subject of intensive research for the last few decades due to the light and abundant elements that can be used—in the case of organic semiconductors—and the flexible nature of these materials. When it comes to semiconductors, a variety of factors such as crystallinity, packing, alignment of orbitals and especially the chemical design govern the overall conductivity of a given material, affecting all of the aforementioned characteristics. Since the introduction of organic electronics, research has moved from self-assemblies of small organic molecules (e.g. pentacene or porphyrins) to large conjugated systems. Pioneering research by MacCullough,[1] Heeger[2] and MacDiarmid,[3] respectively, first lead to conductive polyacetylene and was followed by the design of highly crystalline polythiophenes that upon doping became conductive, thus showcasing the potential of organic materials as lightweight alternatives to silicon. Materials based on the fundamental principles laid out by this early research resulted in highly functional materials that are nowadays employed as organic light-emitting diodes (OLEDs), organic photovoltaics (OPVs) and organic field-effect transistors (OFETs).

Besides the aforementioned factors, dimensionality of the material plays an important role in influencing the performance of the desired product. The most commonly used semiconductor to date is silicon. Silicon crystallizes in a diamond cubic crystal structure and has a narrow band gap. These properties, and the fact that Si can easily be doped to become either electron rich or electron poor, result in a highly functional 3D semiconductor. For Si, a definition of dimensionality is rather straight forward due to the covalent bonds in its crystal structure, but for organic materials such a definition is more nuanced.

In the field of organic electronics this resulted in two commonly used descriptions: (i) the self-assembly of molecules in a bulk solid (e.g. self-assembled discotic liquid crystals of alkyl-substituted porphyrins) and (ii) the π-conjugated domain within a structure (e.g. star-shaped organic molecules). Skabara et al. eloquently addressed these points in a review article by evaluating the different advantages of either concept while also addressing the effect of dimensionality on charge transport.[4] In nanotechnology, on the other hand, dimensionality refers to how many dimensions of a material lie outside of the nano range (1–100 nm). Thus, whereas a C60 fullerene could be considered a 3D semiconductor in the field of organic electronics, in nanotechnology it is a 0D material due to its width being just 0.7 nm. In the following, when referring to dimensionality, unless noted differently, we refer to molecular dimensionality of the discussed nanomaterials.

In this Minireview we will give insights into the development of 2D and 3D porous semiconductors, their design principles and the effect of dimensionality on the electronic conductivity and applications.

1.1. Conduction and the influence of dimensionality in semiconductors

Unlike metals, for which valence electrons extend throughout the crystal lattice, conduction in organic materials is more nuanced, especially when comparing small molecules with 1D polymers and higher dimensional networks. For all of the aforementioned systems, the electronic conductivity is determined by their electronic structure and hence the energy gap between the valence and conduction band. Whereas in small-molecule-based organic semiconductors such as pentacene, charge transport is only possible through the extended π-clouds of perfectly stacked assemblies, in higher dimensional materials—in an ideal scenario—more isotropic charge transport can be the case.[5]

In general, charge transport in solids can be described by two major mechanisms; a hopping mechanism and a band-like mechanism that can be found in materials with strong interactions that enable the material to form a continuous energy band. Whereas in the former case, charges can be transferred

[a] *P. W. Fritz, Prof. A. Coskun*
Department of Chemistry
University of Fribourg
Chemin du Musée 9, 1700 Fribourg (Switzerland)
E-mail: ali.coskun@unifr.ch
The ORCID identification number(s) for the author(s) of this article can be found under:
https://doi.org/10.1002/chem.202005167.

Selected by the Editorial Office for our Showcase of outstanding Review-type articles (www.chemeurj.org/showcase).

between discrete nonbonded sites where these charges reside, in the latter case, charges are delocalized and form an energy band. Since organic and metal–organic semiconductors are often of low symmetry, a temperature dependent hopping-type mechanism should be expected.[6]

It is well known that crystallinity has a tremendous effect on the electronic conductivity of a material. The development of organic electronics based on lower dimensional nanomaterials resulted in a variety of methods driven by non-covalent interactions to improve crystallinity. Techniques such as sublimation or side-chain functionalization to induce self-assembly of polymers (e.g. P3HT[1]) can improve crystallinity but can in some cases also result in polycrystalline materials, undesirable due to abundant grain boundaries. In covalently linked higher dimensional 2D/3D nanomaterials these developments are still ongoing, and most framework-type materials are obtained as polycrystalline powders.

Many ordered 2D and 3D nanomaterials, however, possess one major advantage over lower dimensional systems, that is their ordered porosity. This feature can have a significant effect on charge separation and charge transport properties. The effect of higher dimensionality on charge separation in bulk semiconductors has been heavily studied, especially in the case of OPVs. Findings by Gregg concluded that although entropy has no effect on 1D materials such as columnar assemblies of discotic liquid crystals, this does not hold true in 2D and 3D systems.[7] Here, the electron has an increasing number of states available to it and can move further from its bound positive charge. Hence, charge separation in higher dimensional systems becomes easier since the entropy decreases the barrier of charge separation. Furthermore, 2D and 3D systems have an inherent advantage over lower dimensional systems in their more isotropic charge transport behavior. These findings were further discussed in a 2013 Review by Skabara et al. on charge transport properties in assemblies of organic molecules. The authors furthermore pointed out that, although transfer integrals are the highest for assemblies of disk-like molecules and diminish towards 3D systems, the charge transport properties of 2D and 3D systems are significantly better.[4]

2. 2D and 3D Porous Semiconductors

In recent years, porous organic polymers (POPs), covalent organic frameworks (COFs) and metal–organic frameworks (MOFs) have shaped materials science research due to their structural tunability, large surface areas and plethora of possible applications. Besides finding use in several exciting applications such as gas capture and separation, catalysis and membranes, this group of porous materials sparked special interest for their semiconducting properties and hence their use in organic electronics and photocatalysis. Considering the above-mentioned guidelines for high electronic conductivity, especially crystalline 2D COFs and MOFs are prime candidates for porous semiconductors. Nonetheless, both POPs and 3D COFs also show intriguing properties that if exploited properly result in highly functional materials.

2.1. Semiconducting 2D COFs

The highly ordered structure of 2D COFs as well as their 2D lateral conjugation are intriguing when designing polymers with high charge mobility. Furthermore, the highly crystalline nature of COFs could, in principle, diminish problems commonly found in 1D polymers or POPs originating from chain termination, defects or disorder. Due to that and depending on the chemical moieties chosen in the COF design, two major possibilities for charge transport come to mind. On the one hand, charges can be transferred via the extended π-conjugated systems in similar ways to lower dimensional organic electronic materials such as polythiophenes. The ordered structures and pores on the other hand allow intermolecular charge transport throughout the channels due to the vast degree of interlayer π–π stacking commonly observed in 2D COFs. In the following section we will discuss how different design choices affect the overall conductivity and the interplay between inter- and intramolecular charge transport.

Generally, linkages obtained via condensation reactions involve heteroatoms and hence induce polarized linkages, which affect the stacking behavior and overall electronic properties of the system.[8] Among the most well-known 2D COFs that only exhibit intramolecular charge migration via π–π stacking are boroxine- and boronate-ester-based COFs. In 2005, Yaghi et al. introduced these COFs as they show excellent reversibility in the bond formation and hence high crystallinity in the final structures.[9] However, due to the highly polarized nature of the linkages, charge migration throughout the backbone is

Patrick W. Fritz obtained bis BSc in technical chemistry from Technische Universität Wien (TU Wien) in 2018 and received his MSc from the institute of materials chemistry and the institute of applied synthetic chemistry (IMC and IAS) under the supervision of Prof. Miriam M. Unterlass in 2019. In 2020 he joined the group of Prof. Ali Coskun at University of Fribourg, where he works on porous organic polymers and covalent organic frameworks for separation and energy applications.

Ali Coskun received his PhD degree in chemistry from Middle East Technical University, Ankara, Turkey. He then joined the laboratory of Prof. J. Fraser Stoddart as a postdoctoral research associate at Northwestern University, where he developed dynamic metal–organic frameworks, artificial molecular machines. He started his independent career at Korea Advanced Institute of Science in Technology in 2012. In 2017, he moved to University of Fribourg, Switzerland as a professor. He is currently developing porous organic polymers for CO_2 capture, separation and conversion as well as supramolecular polymers for Li-ion batteries.

almost impossible. Charge migration between the van der Waals stacked, aromatic domains is favored in these highly crystalline COFs. Jiang et al. reported the first photoactive boroxine-based COF by polymerizing pyrene diboronic acid under solvothermal conditions and demonstrated the luminescence properties of the obtained product as well as the on–off ratio of cast COF films.[10] By combining a triphenylene-based core with a porphyrin-based linker, Bein et al. prepared a donor–acceptor framework that formed an internal heterojunction and resulted in one of the first COFs used as an active material in an OPV (Figure 1).[11] Based on these findings, donor–acceptor COFs were designed by post polymerization modification of an azide functionalized COF, which resulted in a framework bearing C60 fullerenes in its pores and thus enabling a covalently bound heterojunction inside the pores of a framework.[12] Sulfur containing building blocks have been heavily exploited in conducting polymers and a substantial amount of research has been conducted on using heavier chalcogens such as Se or Te to further tune the properties of the desired product. Dincă et al. realized the potential of such polymers for framework-based organic photovoltaics and prepared a series of COFs based on substituting sulfur in a benzodithiophene building block with Se and Te. They showed that the heavier chalcogens exhibited increasing conductivity with increasing size. Interestingly, the Te-derived COF featured the highest conductivity ($\sigma = 1.3 \times 10^{-7}\,S\,cm^{-1}$) although showing significantly lower surface area and lower crystallinity compared to the other COFs in the series.[13] Chen et al. reported that large exciton diffusion in COFs is possible in specifically designed boronate-ester-linked COFs, but also pointed out that the lack of a suitable chromophore in their system limited its capability for long-range exciton motion due to the rapid excimer conversion.[14] Bein et al. found that charge-carrier transport is often limited in the bulk, rather than at the COF/electrode interface, indicating that the influence of defects within the COF layers can be detrimental. This holds true especially as the electronic barriers imposed by the boronate ester linkages do not allow charges to evade these defects resulting in the aforementioned reduced charge transport.[15] More recently, Medina et al. were able to design a boroxine-based 2D COF with an electrical conductivity of $2.2 \times 10^{-6}\,S\,cm^{-1}$, which is to our knowledge, the best performing boroxine-based COF. Based on the donor–acceptor strategy, a COF bearing alkyl-functionalized diketopyrrolopyrrole was prepared to probe the influence of crystallinity on the electrical conductivity of the obtained frameworks. In addition, the authors also pointed towards the highly anisotropic electrical conductivity in pressed pellets originating from the random orientation of crystalline phases and the associated grain boundaries within a pressed pellet. Evaluating both materials, namely, crystalline and amor-

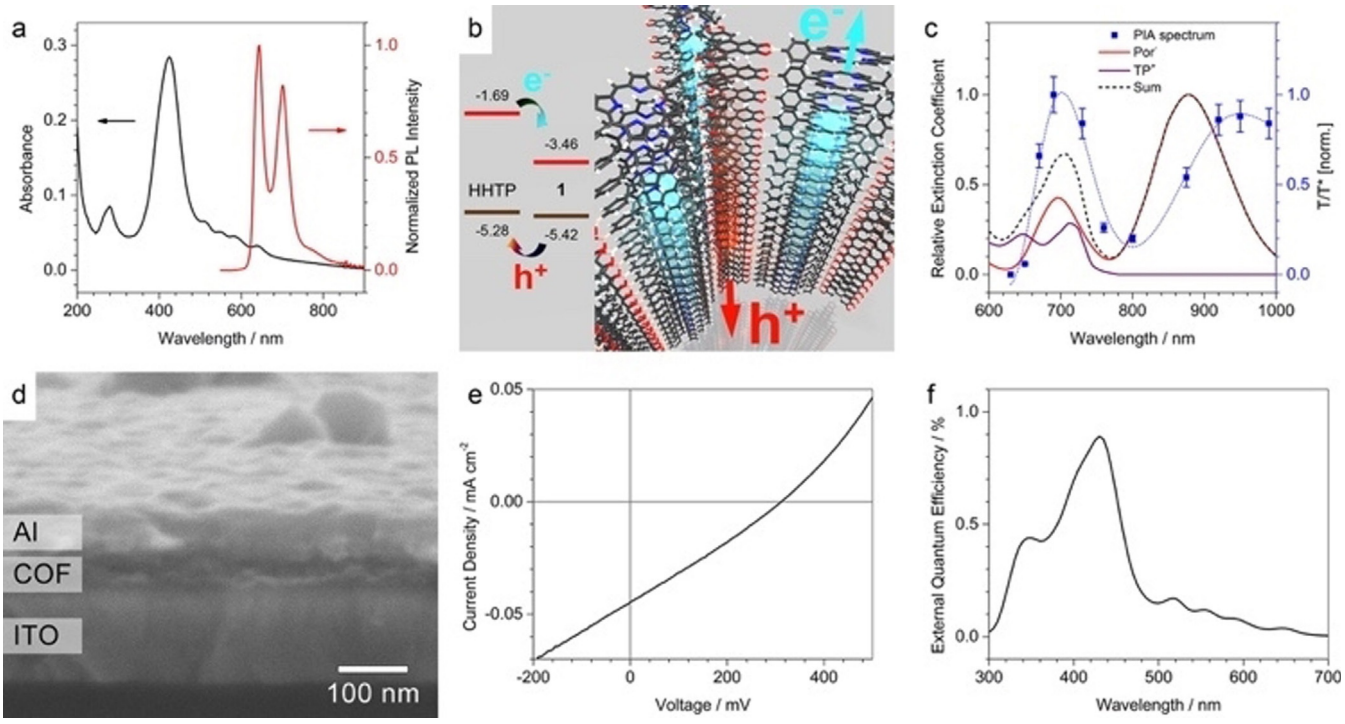

Figure 1. a) Transmission absorption (black) and normalized PL ($\lambda_{exc} = 405$ nm, red) spectra of a TP-Por COF thin film. b) Frontier orbital energies of the two COF subunits measured by DPV in solution and a schematic illustration of the photoinduced charge transfer. c) PIA spectrum of the TP-Por COF film after excitation at 470 nm (blue squares; the blue line serves as a guide to the eye) together with the radical ion absorption spectra of Por^- (red) and TP^+ (purple) and their sum (black) assuming a 1:1 ratio of the two species. After photoexcitation, the TP-Por COF film shows two absorption bands in the range of the free radical ion absorption, indicating electron transfer from the donor to the acceptor moiety within the network (see the text). d) Cross-sectional scanning electron micrograph of a TP-Por COF-based photovoltaic device showing the COF layer between the ITO and Al electrodes. The MoO_x and ZnO contact layers are too thin to be visible in the micrograph. The current–voltage curve (e) and EQE spectrum (f) confirm the successful integration of the donor–acceptor COF as the active layer of the photovoltaic device. Reprinted with permission from Ref. [11].

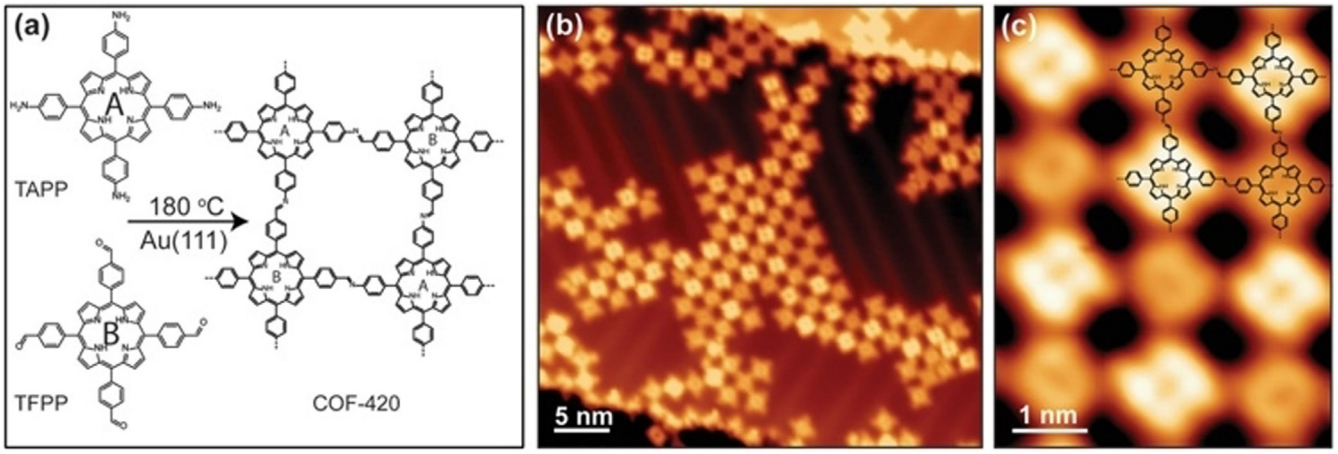

Figure 2. Bottom-up fabrication of COF-420. a) Schematic representation of the synthesis of COF-420 from molecular precursors TAPP and TFPP. b) Representative large-scale STM topographic image of COF-420 on Au(111) (sample bias $V_s = 0.8$. V, tunnel current $I_t = 10$ pA). c) Close-up STM image of COF-420 with the chemical structure overlaid in the top-right corner ($V_s = 0.8$ V, $I_t = 10$ pA). Reprinted with permission from Ref. [17].

phous frameworks, they concluded that the conduction mechanism within COFs can be very similar to that of amorphous systems provided that a homogeneous conduction channel throughout the network is present.[16]

In terms of conductivity, imine-based COFs on the other hand are a borderline case. Although an imine linkage is polarized, the fact that the linker is conjugated means that electrons can—at least in principle—migrate within the lateral plane. Crommie et al. showed the effect of polarized linkages by synthesizing a COF based on porphyrin cores featuring either amine or aldehyde functional groups. After preparing a single layer COF-420 on a gold surface, the electronic structure of the material was evaluated by scanning tunneling microscopy (STM) and revealed that the valence and conduction band were separated through the imine linkages onto the different cores (Figure 2).[17] A Zn-based version of COF-420, TAPP-TFPP-COF, was used to prepare thin films of the conductive COFs, which were used to build a highly sensitive NIR detection device.[18] A major disadvantage of framework materials, in general, is their insolubility. Hence, the processability of COFs to obtain smooth films with high crystallinity is still a subject of research. Ma et al. eloquently circumvented this problem by incorporating charged pyridyl moieties in their imine-based framework, thus creating a COF that could be dissolved in solvents such as NMP or DMF. Although, the high boiling points of these solvents makes conventional casting or printing techniques to obtain smooth films tedious, the fact that the framework self-exfoliated in solution and thin films of rather high conductivity could be obtained is intriguing.[19] Besides porphyrins and phthalocyanines, salphen-based COFs are another intriguing class of metal-containing conductive COFs. Gu et al. recently reported the effect of different oxidation states of the metal complex within the salphen-COFs and showed that going from Ni^{2+} to Ni^0 resulted in a significantly reduced electrical conductivity, adding yet another variable when designing electronically conductive 2D COFs. Thin films of the salphen-based Ni-COF showed an exceptionally high conductivity of 1.2 $S\,cm^{-1}$.[20]

As imine-based COFs are among the most widely studied systems, researchers have come up with a variety of means to improve the electronic conductivity of such systems. The strategy employed by Liu et al. was to integrate functionalities commonly found in 1D organic semiconductors by employing building blocks such as tetrathiafulvalene (TTF), which is an excellent electron donor. As a small molecule or a linear polymer, TTF can form highly conductive charge-transfer crystals. The obtained TTF-COF featured excellent crystallinity and upon doping exhibited a conductivity of 2.8×10^{-3} $S\,cm^{-1}$ and 1.0×10^{-5} $S\,cm^{-1}$ 48 h after doping (Figure 3).[21] Dichtel et al. chose a different approach, that is the electropolymerization or oxidative coupling of 3,4-ethylenedioxythiophene (EDOT) in a redox active imine-based COF, thus inducing high intrinsic conductivity within the pores via highly conductive in situ formed poly(3,4-ethylenedioxythiophene) PEDOT. As expected, both of these approaches resulted in a significant loss of surface area. Nonetheless, these strategies resulted in intriguing composites with high chemical and thermal stability, while also being suitable as electrode materials in Li-ion batteries with a fast-charging capability.[22] Based on the same approach (combining redox active COFs with conductive polymers) Awage et al. prepared a PEDOT@AQ-COF composite material by the solid-state polymerization of brominated EDOT within the pores of a COF.

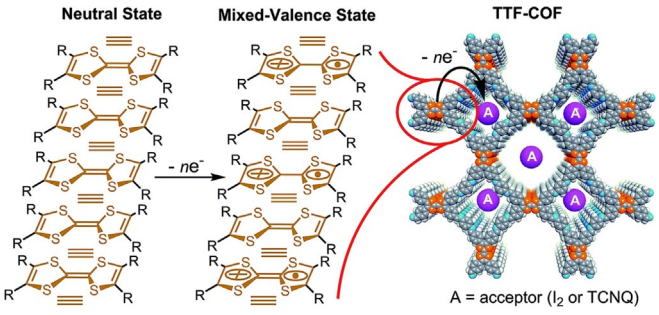

Figure 3. Illustration of the mixed-valence state in TTF-COF. The "≡" indicates inter-TTF-layer interactions. Reprinted with permission from Ref. [21].

This approach allowed them to dope the framework with significantly higher amounts of PEDOT compared to the previously reported approaches, thus enhancing the conductivity by several orders of magnitude (1.1 $S\,cm^{-1}$) and almost reaching the bulk conductivity of crystalline PEDOT.[23] As shown before, utilizing electroactive building blocks in COFs is a quite common strategy, which was further exploited by Perepichka et al. by using azatriangulene as a key building block to obtain a highly conductive COF with interesting magnetic properties.[24] Recently, Fischer et al. reported an approach to increase the in-plane conductivity of COFs by using functionalized graphene nanoribbons (GNRs), which are small, well defined strips of highly conductive graphene, as a backbone and crosslinking them via imine linkages, thus creating highly conductive imine-linked GNR-COFs. Although, no conductivity data was reported, the initial analysis revealed that the combination of fine-tuned bottom-up synthesized GNRs combined with suitable linkers can result in highly conductive 2D COFs with in plane and out of plane conductivity.[25] Using a Michael-type addition and elimination reaction, Bojdys et al. were able to prepare a β-amino enone-linked framework that showed fast and highly sensitive response in its electrical conductivity and optical properties based on the chemisorption or cleavage of protons, showcasing the usability of this material as a chemical sensor.[26] Recently, Bein et al. showcased the influence of film orientation on the electrical conductivity in an imine-based framework. Their study showed that besides the orientation of the film, the quality of surface of the COF film played a crucial role in relation to the measurement geometry. Interestingly, for the doped samples (e.g. iodine and $SbCl_5$), the orientation of the film played only a minor role. This is a rather intriguing observation, which indicates the necessity of structural characterization of COFs following doping to establish structure–property relationships.[27]

Due to the limitations associated with boroxine and imine COFs, or polarized COF linkages in general, efforts have been made to create highly crystalline phenazine or carbon linked systems, thus avoiding these highly polarized linkages. The first sp^2-linked COF was prepared via Knovenagel condensation and resulted in a highly crystalline nitrile-bearing framework that showed high potential as a supercapacitor.[28] By employing the same strategy, Jiang et al. reported a 2D COF linked via cyanovinylene units. Although fully conjugated, the COF showed no electrical conductivity in its undoped state, which can be attributed to the lack of charge carriers. This was subsequently solved by doping the COF with iodine, which led to a significant increase in conductivity (7.1×10^{-4} $S\,cm^{-1}$).[29]

In 2019, Zhang et al. reported the preparation of a vinylene-linked sp^2-COF and showcased its semiconducting properties by utilizing the framework as a photocatalyst for the hydrogen evolution reaction (HER). Although, the COF could be used as a photocatalyst without using any precious metals, the hydrogen evolution rate was significantly better upon using Pt as a cocatalyst.[30] Using the copper surface to act as a template and catalyst simultaneously, Bojdys et al. prepared a crystalline 2D polymer film accompanied by a 3D amorphous phase. The polymer obtained via a cyclotrimerization of terminal alkyne units showed an internal donor–acceptor structure and was used as a heterogeneous photocatalyst for HER. Interestingly, the authors established that the microporosity found in the open framework structure of the amorphous 3D TzG film facilitated the photocatalytic reaction while the crystalline 2D film helped supporting the TzF/TzG composite.[31] Phenazine-linked COFs are another intriguing class of frameworks that enable full 2D conjugation, thus facilitating a platform for highly porous materials that can be exploited as hole conducting materials with high charge carrier mobility.[32] Fully conjugated, phenazine-linked phtalocyanine COFs reported by Mirica et al. showed promise as gas sensing materials and electroactive COFs due to the increased orbital interaction between the layers and the presence of a donor–acceptor motif commonly found in conventional 1D polymers.[33] Another intriguing 2D semiconductor-based on phenazine linkages was reported by Liu and co-workers. They managed to optimize the synthetic conditions in the formation phenazine linkages to allow full reversibility in order to obtain a highly crystalline fully conjugated COF that featured a conductivity of 3×10^{-5} $S\,cm^{-1}$. Based on the high redox stability of the framework together with the internal electrical conductivity, it was successfully employed as a cathode material in lithium-ion batteries.[34] The authors clearly showed that the electrode performance of the crystalline framework is significantly better than its amorphous counterpart. This result can be attributed to the availability of ordered channels, which enabled efficient charging and discharging. It should, however, be noted that imparting a framework material or composite with electrical conductivity also significantly enhances the overall performance as a cathode material, which was recently shown by Coskun and co-workers.[35]

Especially for electronic applications, uniform surfaces/interfaces are preferred over polycrystalline powders to reduce losses originating from structural defects and grain boundaries. Yet, a majority of frameworks are obtained as polycrystalline powders of different particle sizes and are pressed to pellets to conduct conductivity measurements. To avoid losses originating from grain boundaries and defects a variety of methods have been developed including the deposition of the building blocks under vacuum onto a substrate where they are polymerized,[36] exfoliation[37] or interfacial polymerization.[25,38] Among them, interfacial polymerization has been employed heavily due to the possibility of obtaining large area thin films. Recently, methods to obtain single crystalline COFs such as seeded growth[39] or tuned reversibility[40] have been reported, thus showcasing the possibility to obtain highly crystalline 2D and 3D COFs. Whereas these methods enable researchers to prepare conductive thin films on a lab-scale basis, further development is required in order to bring these technologies to an industrially applicable point.

2.2. Semiconducting POPs

Porous organic polymers, POPs, have been extensively studied due to their ease of synthesis, high surface areas, high physical, chemical and thermal stability and especially in the case of carbonized POPs their high electrical conductivity. Although they

lack crystallinity, the fact that most POPs are linked via C–C bonds, present conductivities comparable to the COFs and MOFs. POPs are conventionally synthesized under kinetically controlled reaction conditions and result in the formation of irreversible bonds. Whereas COFs and MOFs are based on reversible bonds and result in the formation of a thermodynamic product, POP syntheses mostly yield the kinetic product. Synthetic strategies to design and tune the band gap of POPs often revolve around the incorporation of conjugated linkers. Although this often results in the desired effect, increasing the spacer length can simultaneously promote framework interpenetration.[41] Due to the disadvantages associated with the lack of crystallinity in relation to electronic conduction, a majority of research in the field of POPs has focused on utilizing the high stability and (micro)porosity of these materials for heterogeneous catalysis and especially for photocatalytic hydrogen evolution reaction.[42] A prime example of such a heavily investigated 2D material is triazine-based graphitic carbon nitride, a material often compared to graphene. Bojdys et al. investigated the highly anisotropic charge transport in such systems by measuring in-plane, out of plane and bulk conductivity showcasing, the effect of grain boundaries and the associated increased contact resistance.[43]

Donor–acceptor motifs are commonly applied in POPs. Bojdys et al. showcased the potential of tuning the D–A strength and interactions by employing sulfur and nitrogen containing building blocks. The obtained materials showed excellent photocatalytic activity and showcased the impact of fine-tuning of the band gaps in polymers (Figure 4).[41,44] The group also showed that a lack of order inhibits exciton annihilation by preparing both the kinetic and the thermodynamic product of the same material and investigating the effect on the conductivity and photocatalytic performance of the materials.[45]

Coskun et al. reported a different approach towards fine-tuning band gaps. A carefully designed precursor allowed to tune band gaps by enabling an intramolecular cyclization depending on the strength of the acid catalyst utilized during the synthesis. Interestingly, the procedure not only affected the band gap of the materials, but also their surface area in a linear and reproducible fashion.[46]

POPs are intriguing platforms to derive highly conductive materials, which was nicely demonstrated by Dong and coworkers.[47] The authors prepared conjugated microporous polymers via Suzuki–Miyaura coupling reaction and subsequently carbonized the obtained polymers to obtain porous carbon nanoparticles with high electrical conductivity of up to 22 $S\,cm^{-1}$. Although these results are impressive, carbonized polymers are not conventionally employed in organic electronics due to their problematic processing and the overall rather anisotropic properties. In an attempt to synthesize a 3D framework, Li et al. employed highly conductive polythiophene units as linkers and were able to obtain POPs with intriguing conductivities reaching up to 2.1×10^{-3} $S\,cm^{-1}$. Interestingly, the longer polythiophene linker showed lower conductivities, but higher overall capacity and coulombic efficiency when used as an electrode material in Li-ion batteries.[48] Also by utilizing a monomer bearing a sp^3-core, Börjesson et al. developed a continuous flow method based on non-reversible coupling chemistry to prepare smooth continuous films 3D POPs.[49] In an attempt to overcome the necessity of sp^3 carbons and coupling chemistry in all-organic 3D semiconductors, Coskun et al. recently demonstrated the preparation of epoxide-bearing 3D POPs via the Diels–Alder cycloaddition polymerization, which was subsequently aromatized to form a first example of a fully sp^2-hybridized 3D graphitic porous polymer. Upon aromatization, besides an increase in the surface area, an immediate increase (two orders of magnitude) in the conductivity could be measured, which could be further improved by I_2 doping to 6×10^{-4} $S\,cm^{-1}$ (Figure 5).[50]

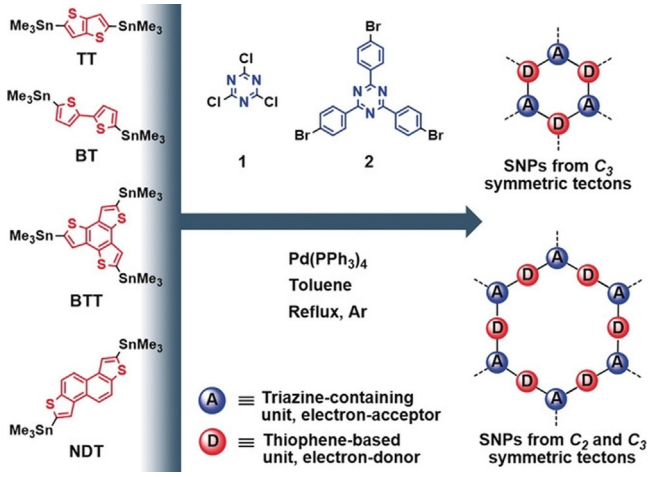

Figure 4. Synthetic pathway toward sulfur and nitrogen containing porous polymers (SNPs). C_2 and C_3 symmetric thiophene-based electron-acceptors (in red) are coupled with C_3 symmetric triazine containing electron acceptors (in blue). Reprinted with permission from Ref. [44].

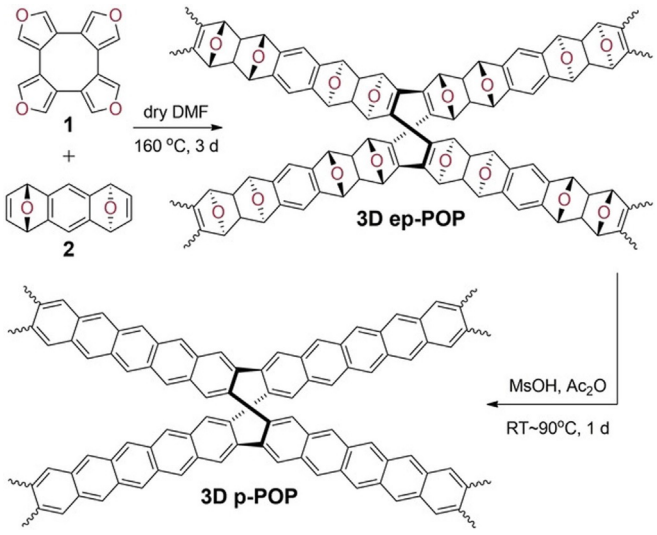

Figure 5. Synthesis of 3D ep-POP via Diels–Alder cycloaddition polymerization of **1** and **2** followed by methanesulfonic acid promoted and acetic anhydride-promoted cyclodeoxygenation to form 3D p-POP. Reprinted with permission from Ref. [50a].

2.3. Semiconducting 3D COFs

The majority of COFs found in the literature are 2D networks, mainly due to the increased complexity when moving towards 3D systems. On the one hand, the range of feasible building blocks is limited and often involves sp^3 carbon centers that break conjugation (e.g. tetraphenylmethane or adamantanes), thus reducing the overall conductivity of the framework. On the other hand, the synthetic procedures have to be even more optimized in order to obtain highly crystalline, non-interpenetrated 3D frameworks to ensure high charge mobility. It should be noted that interpenetrated systems are by no means undesirable as they result in closer packing of the molecules and in some cases increased overall interactions. Qiu et al. synthesized a mostly crystalline electroactive 3D COF via a Yamamoto-type Ullmann coupling from a simple halide precursor on a rather large scale. The triphenylamine-based framework is redox active and although it became electrically conductive upon I_2 doping, it showed rather low charge carrier concentrations due to its open framework structure.[51] A porphyrin-based photocatalyst was prepared by Wang et al. that utilized the photophysical properties of the building block and showed the detrimental effect of a metal center, that is, paramagnetic metals such as Cu in the porphyrin on the photochemical performance.[52] In a similar fashion to the previously reported 2D COFs, Fang et al. utilized tetrathiafulvalene as a building block to enhance the conductivity and to obtain frameworks with very high surface areas of up to 3000 $m^2 g^{-1}$. Although, the frameworks employed a TTF unit—often used in highly conductive 1D polymers—the materials showed rather low conductivities, which could, however, be significantly enhanced by iodine doping to reach up to 1.4×10^{-2} $S cm^{-1}$. These results are particularly interesting as the 3D TTF-COFs outperform the corresponding 2D COFs (e.g. TTF-COF(I2) 1.0×10^{-5} $S cm^{-1}$), which can partly be attributed to the higher surface areas and higher iodine retention in the polymers.[53] Wang et al. further contributed to the field of semiconducting 3D COFs by preparing and utilizing a highly luminescent imine-based framework. The framework capable of aggregation-induced emission—that is, the property of a material to be emissive as aggregates—was used as a coating layer for a blue-emitting phosphor, thus creating a white light-emitting diode.[54] The conversion of 2D to 3D frameworks via reversible cycloaddition reaction was first demonstrated by Thomas et al.[55] and was subsequently used by Perepichka et al. to synthesize a 2D framework that could be photochemically crosslinked to form a 3D framework and switched back to the original state upon thermal treatment. Surprisingly, the fully conjugated vinylene linked 2D COF and the cyclobutane-linked 3D COF showed only negligible electrical conductivity. This is especially surprising in the case of the 2D framework as it even features a push–pull system that should result in a decent electronic conductivity and thus pointing to a lack of charge carriers in the undoped state (Figure 6). Even though, the 2D frameworks achieved only low electronic conductivity, they showed very promising proton and Li-ion conductivities, whereas the 3D framework lacked behind in these two metrics as well.[56]

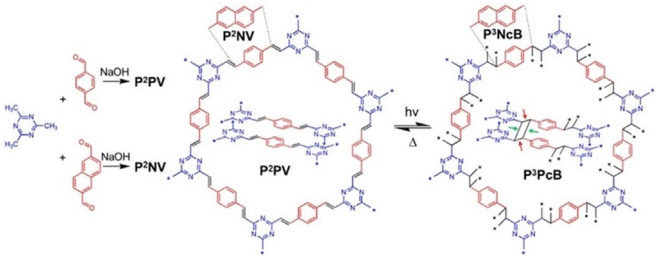

Figure 6. Synthesis of **P²PV** and **P²NV** COFs,(36) their photoinduced [2+2] cycloaddition into **P³PcB** and **P³NcB**, and thermal cycloreversion. Reprinted with permission from Ref. [56].

Very recent approaches showcase the unique advantages of moving from 2D to 3D frameworks, thus further emphasizing the importance of dimensionality. Wang et al. showed the drastic effect of porphyrin stacking on the overall photocatalytic activity of a framework originating from the π–π stacking in 2D frameworks compared to the "designed stacking" in 3D frameworks. Based on their previous study they prepared 2D and 3D frameworks differing only in their amine linker. Employing Pd instead of Cu to reside in the porphyrin core enhanced the photosensitizing properties of their materials. They also concluded that the overall narrower pore size and higher surface area of the 3D framework resulted in better performing photocatalysts (Figure 7).[57]

2.4. Semiconducting MOFs

Among crystalline framework materials, MOFs, in general, feature higher electronic conductivity. A plethora of studies have focused on mechanisms related to charge transport in MOFs. Yet, electrical conduction in MOFs is quite diverse between extremely conductive non-porous MOFs such as Cu_3BHT,[58] that are able to reach conductivities of up to 2500 $S cm^{-1}$ and porous MOFs that show structure and crystallinity depend on properties that range from conductivities comparable to COFs to the conductivity of amorphous silica. Although a significant research progress has been made, a multitude of different conduction mechanisms are plausible for MOFs. Recent, reviews by Dincă et al. and Mirica et al., respectively, provided a comprehensive evaluation of conduction and charge transport mechanism in MOFs, therefore is not covered in this Minireview.[6,59]

3. The Effect of Dimensionality in Porous Semiconductors

Based on the research presented in this Minireview, it is clear that the question of "what kind of influence dimensionality has on porous semiconductors?" cannot be answered unambiguously. Hinging on the research on molecular semiconductors, there is of course an advantage of going from 0D and 1D to higher dimensionality due to the positive entropic effect described by Gregg and the effect on charge separation and migration described by Skabara.[4,7] Both of these can, however, be harnessed by almost all 2D and 3D nanomaterials. Exceptions from this might be boroxine and boronate-ester-linked

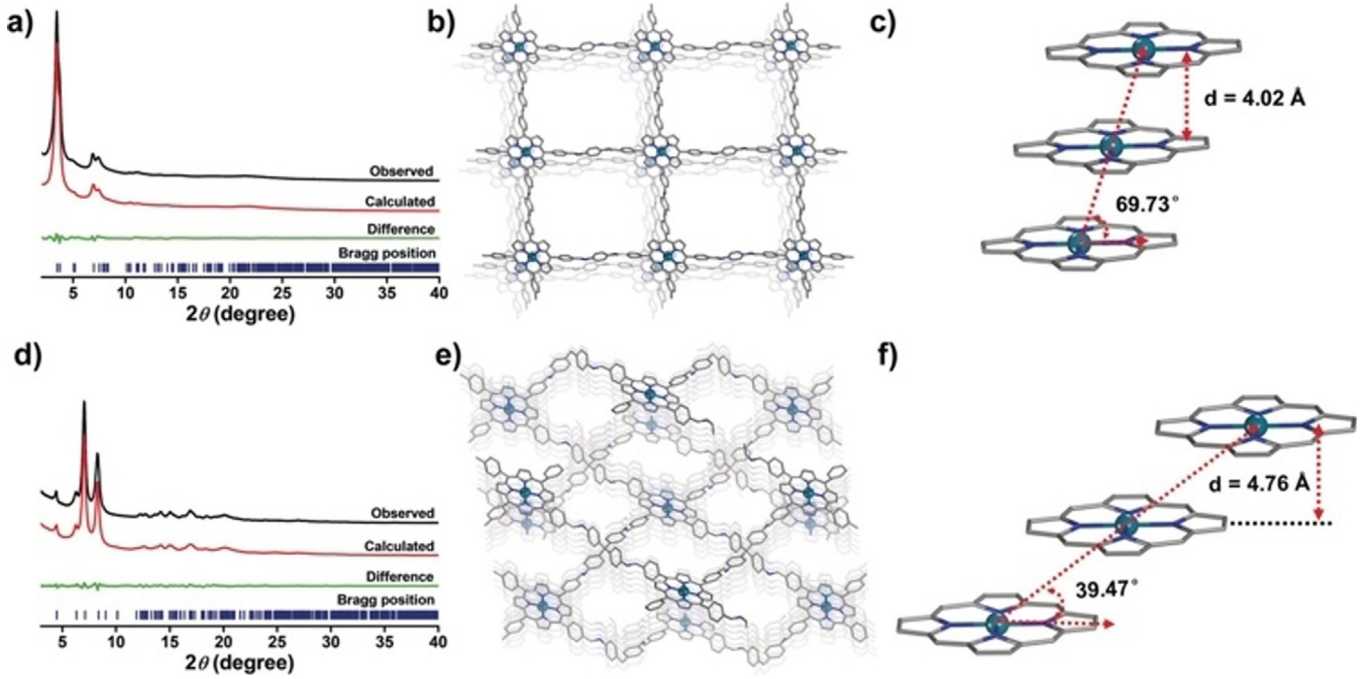

Figure 7. a,d) PXRD patterns of 2D-PdPor-COF (a) and 3D-PdPor-COF (d) with the experimental profiles in black, Rietveld refinement in red, their difference in green, and the Bragg position in blue. b),e) Structural representations of 2D-PdPor-COF (b) and 3D-PdPor-COF (c), in which the former has an eclipsed AA stacking 2D structure and the latter adopts a five-fold interpenetrated pts topology. c),f) Diagrams of the stacking of palladium porphyrin units in 2D-PdPor-COF (c) and 3D-PdPor-COF (f). Reprinted with permission from Ref. [57].

systems as they break conjugation which might nullify these effects. Generally speaking, the wide range of possible applications for porous semiconductors resulted in a highly specialized research, wherein scientists were able to predict design/functionality interactions for specific systems in their field.

Here, we critically evaluated a multitude of porous materials spread over an ever-growing field of applications, all of which benefit from high intrinsic conductivity (see Table 1). Figure 8 clearly shows that it is difficult to establish a direct correlation between higher dimensionality and the associated higher surface area and high electronic conductivity, which is especially true for MOFs, where dense films of highly crystalline materials significantly outperform their porous counterparts. The extent of polymerization, defect density and packing/conjugation of molecular units also play a major role in the overall conductivity. Nevertheless, porosity still plays an important role, for example, whereas many COFs exhibit a very low conductivity in their undoped state, they become highly conductive upon doping due to their large surface areas and the high iodine retention capability within the framework structures. At this point, a clear advantage for 3D COFs could be expected since they generally show higher surface areas and hence higher total iodine uptake and retention (e.g. JUC-Z2 or JUC-518). Although, this is the case for some systems, the fact that vastly fewer conductive 3D frameworks are reported limits the feasibility to draw a clear conclusion. Furthermore, research based on 2D frameworks is far more advanced compared to 3D systems, which can easily be seen by the variety of doping agents (e.g. iodine, conductive polymers, fullerenes etc.). Moreover, research on 2D frameworks greatly profits from the wide range of building blocks such as metal containing salphen units in Ni-COF or units such as tetrathiafulvalene that are commonly found in organic electronics.

Amorphous polymers on the other hand play a very interesting role, often showing similar or higher conductivity compared to their crystalline counterparts, due to their full conjugation, indicating that polarized bonds in COFs are still among the most limiting factors in creating highly conductive semiconductors. Although researchers were recently able to bridge the gap by moving from polarized linkages to non-polarized fully conjugated systems while retaining crystallinity, the obtained frameworks still showed rather low bulk conductivities indicating that the molecular design requires further optimization. Especially in the field of OPVs, POPs with their 3D nanostructures have been heavily investigated due to the possibility to easily induce bulk heterojunctions by doping the systems with fullerenes, thus easing charge separation, while preventing agglomeration of the dopants.[63] Furthermore, the locked geometry of 3D POPs compared to 1D polymers has been reported to reduce orientation issues when conducting electrons/holes.[64] Moreover, research has shown that in the case of photocatalysis, more disordered materials can result in vastly better performance due to reduced exciton annihilation or more abundant functional groups, not consumed during the synthesis.[65] Another factor complicating a clear conclusion is the fact that, although applications such as photocatalysis do generally benefit from higher surface areas, there are still a variety of applications (e.g. OLEDs, OFETs and OPVs) where no direct correlation between high surface area and high performance can be drawn.[42a]

Table 1. Summary of the properties of porous semiconductor including the presence of dopants, crystallinity, electrical conductivity and the associated measurement methods along with BET surface areas.

Material	Description	Crystallinity	σ [S cm^{-1}]	σ Method	BET SA [m^2 g^{-1}]	Ref.
2D COFs						
1-S		*x*	3.7×10^{-10}	two-probe pellet	1424	[13]
1-Se		*x*	8.4×10^{-19}	two-probe pellet	1634	[13]
1-Te		*x*	1.3×10^{-7}	two-probe pellet	352	[13]
DPP2-HHTP- COF		*x*	2.2×10^{-6}	four-point pellet	1000	[16]
DPP2-HHTP- COF	amph.	–	2×10^{-7}	four-point pellet		[16]
PyVg-COF		*x*	4×10^{-3}	film on ITO (v)	348	[19]
PyVg-COF		*x*	1.8×10^{-12}	film on ITO (h)	348	[19]
Ni_0-COF		*x*	8.4×10^{-6}	two-probe pellet	258	[20]
Ni-COF		*x*	1.3×10^{-2}	two-probe pellet	362	[20]
Ni-COF		*x*	1.2	film—van der Pauw	362	[20]
TTF-COF		*x*	1.2×10^{-6}	film on Si/SiO2	720	[21]
TTF-COF	ox (i2)	*x*	1.0×10^{-5}	film on Si/SiO2		[21]
DAAQ-TFP		*x*	4.4×10^{-5}	PEIS	1140	[22a]
DAPH-TFP		*x*	4.8×10^{-5}	PEIS	1155	[22a]
PEDOT@DAAQ- TFP		*x*	7.5×10^{-5}	PEIS	347	[22a]
PEDOT@DAPH- TFP		*x*	7.2×10^{-5}	PEIS	230	[22a]
PEDOT@AQCOF		*x*	1.1	two-probe pellet	131	[23]
AQCOF		*x*	1×10^{-10}	two-probe pellet	1203	[23]
TANG-COF		*x*	1.6×10^{-5} (v)	two-probe pellet	440	[24]
TANG-COF		*x*	5×10^{-12} (h)	two-probe pellet	440	[24]
TANG-COF	ox (I2)	*x*	1×10^{-2}	two-probe pellet	440	[24]
POR-COF		*x*	4.6×10^{-11}	two-probe pellet	447	[60]
POR-COF	ox (I2)	*x*	1.52×10^{-7}	two-probe pellet		[60]
PBHP-TAPT COF		*x*	1.32×10^{-10}	two-probe pellet	176	[26]
PBHP-TAPT COF	H+	*x*	2.18×10^{-8}	two-probe pellet	176	[26]
sp^2c-COF		*x*	6.1×10^{-16}	two-probe pellet	692	[29]
sp^2c-COF	ox (I2)	*x*	7.1×10^{-4}	two-probe pellet		[29]
COF-DC-8		*x*	2.51×10^{-5}	four-point pellet	360	[33]
PGF-1		*x*	3×10^{-5}	Pellet van der Pauw	101	[34]
POPs						
POP-1		–	2.1×10^{-3}	four-point pellet	260	[48]
POP-2		–	6.7×10^{-3}	four-point pellet	342	[48]
CCMP-1	carbonized	–	12.5	four-point pellet	655	[47]
CCMP-2	carbonized	–	22	four-point pellet	607	[47]
CCMP-3	carbonized	–	7	four-point pellet	596	[47]
CCMP-4	carbonized	–	19	four-point pellet	392	[47]
3D ep-POP		–	$8(1)\times10^{-10}$	two-probe pellet	779	[50a]
3D *p*-POP		–	$5(3)\times10^{-8}$	two-probe pellet	801	[50a]
I2@*p*-POP	ox (I2)	–	$6(2)\times10^{-4}$	two-probe pellet		[50a]
I2@*p*-POP, 8 h vacuum	ox (I2) (vac)	–	$2.9(3)\times10^{-5}$	two-probe pellet		[50a]
3D COFs						
JUC-Z2	ox (I2)	–	1×10^{-2} (c)	two-probe pellet		[51]
JUC-518	ox (I2)	*x*	2.9×10^{-7} (*x*)	two-probe pellet		[53]
JUC-518	ox (I2)	*x*	2.7×10^{-4} (*y*)	two-probe pellet		[53]
JUC-519	ox (I2)	*x*	1.8×10^{-7} (*x*)	two-probe pellet		[53]
JUC-519	ox (I2)	*x*	3.4×10^{-4} (*y*)	two-probe pellet		[53]
P^2PV		*x*	1.1×10^{-9}	two-probe pellet	880	[56]
P^3PcB		*x*	1.1×10^{-9}	two-probe pellet	1073	[56]
2D and 3D MOFs						
Y_6HOTP_2		*x*	2.0×10^{-5}	four-point pellet	780	[61]
$Co_3(HITP)_2$		*x*	2.4×10^{-2}	four-point pellet	805	[62]
$Cu_3(HITP)_2$		*x*	7.5×10^{-1}	four-point pellet	495	[62]
$Ni_3(HITP)_2$		*x*	55.4	four-point pellet	885	[62]
Cu_3BHT		*x*	2500	four-point film	dense	[58b]

(h) horizontal; (v) vertical; (*x*) 6 h at 25 °C; (*y*) … 48 h at 120 °C; (c) converted from resistivity using $R=\rho\frac{L}{A}$ with $\sigma=\frac{1}{\rho}$.

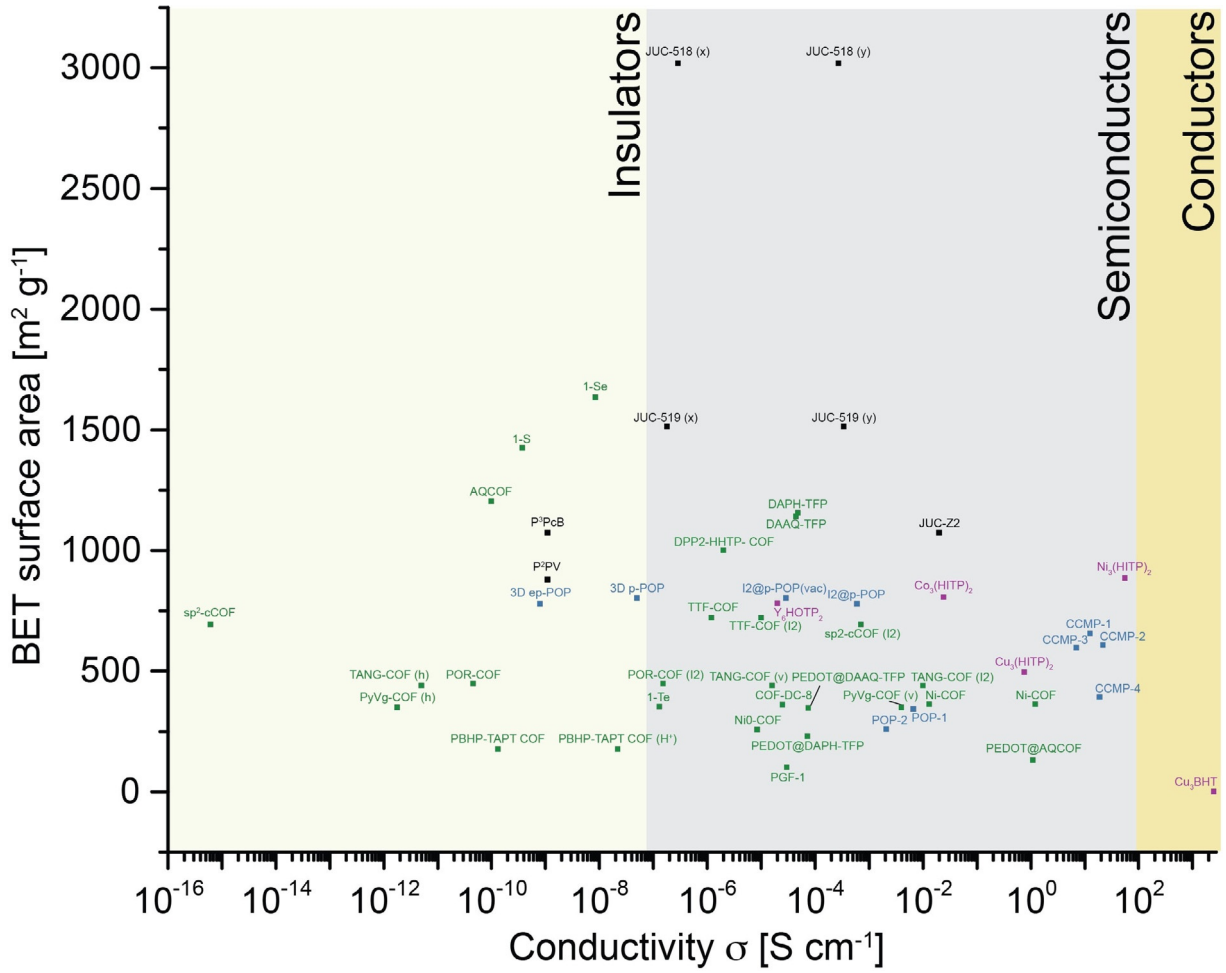

Figure 8. Conductivity of conductive COFs, POPs and MOFs (on a logarithmic scale) plotted against their surface area. Iodine doped COFs were plotted against the surface area of the parent framework, due to a lack of BET-SA data for doped frameworks. Materials classes were highlighted according to 2D COFs (green), POPs (dark blue), 3D COFs (black) and MOFs (light blue). Transitions between insulators, semiconductors and conductors were highlighted—transitions are in accordance to Yoon and co-workers.[66]

4. Summary and Outlook

In recent years, the field of porous semiconductors has significantly diversified. Hinging on the mostly untapped potential of COFs, POPs and MOFs, a plethora of suitable synthetic and post synthetic strategies have been developed to tune and optimize these materials, resulting in a wide range of possible applications. Although, these efforts resulted in an increasingly growing hub of knowledge, most of it is very specific to certain applications, diminishing the possibility to use the gained information in a broader perspective.

Based on the intriguing properties of low-dimensionality semiconductors, researchers envisioned that higher-dimensional materials would reduce problems (e.g. stability and lifetime) associated with lower dimensionality, while increasing charge transport throughout the materials with ordered porosity. In particular, the possibility to trap dopants (e.g. iodine or fullerenes), or even conductive polymers (e.g. PEDOT) in the structure of a framework to create highly functional composite materials shows a great potential resulting in some of the highest herein showcased bulk conductivities (PEDOT@AQCOF, 1.1 $S\,cm^{-1}$). Although, a variety of studies have shown that this is indeed the case, the chemical design of the material is still the main driving force governing electrical conduction. Another interesting factor is the dimensionality of the material, which has so far, not received a lot of attention. This lies in stark contrast to molecular semiconductors, where the dimensionality and the associated effect on charge transport and charge separation have been heavily studied. Although, most 2D and 3D nanomaterials share the positive effects, associated with moving from lower dimensionality to higher dimensionality from a molecular point of view, the chemical design choices are likely to impact the degree to which these effects can be harnessed.

Ultimately, the case for dimensionality in porous semiconductors is not a trivial one. The fact that different applications require different combinations of high intrinsic conductivity, high surface area, high micropore volume etc. makes it rather challenging to draw a clear line. Moreover, well-known inorganic semiconductors such as silicon cannot be used as models for porous organic materials as the comparable chemical design would ultimately lead to non-conjugated materials,

thus lacking electrical conductivity. Nonetheless, key studies such as the work presented by Wang and co-workers, clearly show the positive effect when moving to higher dimensionality.[57]

Overall, higher dimensionalities not only facilitate more isotropic charge transfer given a suitable chemical design, but also provide a porous structure that can be leveraged for a variety of applications that profit from well-defined pores and high surface areas. The advent of single crystalline COFs and MOFs and the increased interest in the topic could significantly drive the field towards a deeper understanding of dimensionality. We believe that the interplay between dimensionality, conductivity and surface area is crucial in designing novel, highly functional materials and should be considered in designing porous semiconductors.

Acknowledgements

A.C. thanks the Swiss National Science Foundation (SNSF) for funding of this research (200021-175947).

Conflict of interest

The authors declare no conflict of interest.

Keywords: covalent organic frameworks · dimensionality · organic semiconductors · porous organic polymers · porous semiconductors

[1] R. D. McCullough, *Adv. Mater.* **1998**, *10*, 93 – 116.
[2] A. J. Heeger, *Chem. Soc. Rev.* **2010**, *39*, 2354 – 2371.
[3] A. G. MacDiarmid, R. J. Mammone, R. B. Kaner, L. Porter, R. Pethig, A. J. Heeger, D. R. Rosseinsky, R. J. Gillespie, P. Day, *Philos. Trans. R. Soc. London Ser. A* **1985**, *314*, 3 – 15.
[4] P. J. Skabara, J. B. Arlin, Y. H. Geerts, *Adv. Mater.* **2013**, *25*, 1948 – 1954.
[5] a) P. Parisse, M. Passacantando, S. Picozzi, L. Ottaviano, *Org. Electron.* **2006**, *7*, 403 – 409; b) V. Coropceanu, H. Li, P. Winget, L. Zhu, J.-L. Brédas, *Annu. Rev. Mater. Sci.* **2013**, *43*, 63 – 87.
[6] L. S. Xie, G. Skorupskii, M. Dinca, *Chem. Rev.* **2020**, *120*, 8536 – 8580.
[7] B. A. Gregg, *J. Phys. Chem. Lett.* **2011**, *2*, 3013 – 3015.
[8] D. D. Medina, T. Sick, T. Bein, *Adv. Energy Mater.* **2017**, *7*, 1700387.
[9] A. P. Côté, A. I. Benin, N. W. Ockwig, M. O'Keeffe, A. J. Matzger, O. M. Yaghi, *Science* **2005**, *310*, 1166 – 1170.
[10] S. Wan, J. Guo, J. Kim, H. Ihee, D. Jiang, *Angew. Chem. Int. Ed.* **2009**, *48*, 5439 – 5442; *Angew. Chem.* **2009**, *121*, 5547 – 5550.
[11] M. Calik, F. Auras, L. M. Salonen, K. Bader, I. Grill, M. Handloser, D. D. Medina, M. Dogru, F. Lobermann, D. Trauner, A. Hartschuh, T. Bein, *J. Am. Chem. Soc.* **2014**, *136*, 17802 – 17807.
[12] L. Chen, K. Furukawa, J. Gao, A. Nagai, T. Nakamura, Y. Dong, D. Jiang, *J. Am. Chem. Soc.* **2014**, *136*, 9806 – 9809.
[13] S. Duhović, M. Dincă, *Chem. Mater.* **2015**, *27*, 5487 – 5490.
[14] N. C. Flanders, M. S. Kirschner, P. Kim, T. J. Fauvell, A. M. Evans, W. Helweh, A. P. Spencer, R. D. Schaller, W. R. Dichtel, L. X. Chen, *J. Am. Chem. Soc.* **2020**, *142*, 14957 – 14965.
[15] D. D. Medina, M. L. Petrus, A. N. Jumabekov, J. T. Margraf, S. Weinberger, J. M. Rotter, T. Clark, T. Bein, *ACS Nano* **2017**, *11*, 2706 – 2713.
[16] S. Rager, A. C. Jakowetz, B. Gole, F. Beuerle, D. D. Medina, T. Bein, *Chem. Mater.* **2019**, *31*, 2707 – 2712.
[17] a) T. Joshi, C. Chen, H. Li, C. S. Diercks, G. Wang, P. J. Waller, H. Li, J. L. Bredas, O. M. Yaghi, M. F. Crommie, *Adv. Mater.* **2019**, *31*, 1805941; b) C. Chen, T. Joshi, H. Li, A. D. Chavez, Z. Pedramrazi, P. N. Liu, H. Li, W. R. Dichtel, J. L. Bredas, M. F. Crommie, *ACS Nano* **2018**, *12*, 385 – 391.
[18] X. Xu, S. Wang, Y. Yue, N. Huang, *ACS Appl. Mater. Interfaces* **2020**, *12*, 37427 – 37434.
[19] L. Wang, C. Zeng, H. Xu, P. Yin, D. Chen, J. Deng, M. Li, N. Zheng, C. Gu, Y. Ma, *Chem. Sci.* **2019**, *10*, 1023 – 1028.
[20] T. Li, W.-D. Zhang, Y. Liu, Y. Li, C. Cheng, H. Zhu, X. Yan, Z. Li, Z.-G. Gu, *J. Mater. Chem. A* **2019**, *7*, 19676 – 19681.
[21] S.-L. Cai, Y.-B. Zhang, A. B. Pun, B. He, J. Yang, F. M. Toma, I. D. Sharp, O. M. Yaghi, J. Fan, S.-R. Zheng, W.-G. Zhang, Y. Liu, *Chem. Sci.* **2014**, *5*, 4693 – 4700.
[22] a) E. Vitaku, C. N. Gannett, K. L. Carpenter, L. Shen, H. D. Abruña, W. R. Dichtel, *J. Am. Chem. Soc.* **2020**, *142*, 16 – 20; b) C. R. Mulzer, L. Shen, R. P. Bisbey, J. R. McKone, N. Zhang, H. D. Abruna, W. R. Dichtel, *ACS Cent. Sci.* **2016**, *2*, 667 – 673.
[23] Y. Wu, D. Yan, Z. Zhang, M. M. Matsushita, K. Awaga, *ACS Appl. Mater. Interfaces* **2019**, *11*, 7661 – 7665.
[24] V. Lakshmi, C. H. Liu, M. Rajeswara Rao, Y. Chen, Y. Fang, A. Dadvand, E. Hamzehpoor, Y. Sakai-Otsuka, R. S. Stein, D. F. Perepichka, *J. Am. Chem. Soc.* **2020**, *142*, 2155 – 2160.
[25] G. Veber, C. S. Diercks, C. Rogers, W. S. Perkins, J. Ciston, K. Lee, J. P. Llinas, A. Liebman-Peláez, C. Zhu, J. Bokor, F. R. Fischer, *Chem* **2020**, *6*, 1125 – 1133.
[26] R. Kulkarni, Y. Noda, D. Kumar Barange, Y. S. Kochergin, P. Lyu, B. Balcarova, P. Nachtigall, M. J. Bojdys, *Nat. Commun.* **2019**, *10*, 3228.
[27] J. M. Rotter, R. Guntermann, M. Auth, A. Mähringer, A. Sperlich, V. Dyakonov, D. D. Medina, T. Bein, *Chem. Sci.* **2020**, *11*, 12843 – 12853.
[28] X. Zhuang, W. Zhao, F. Zhang, Y. Cao, F. Liu, S. Bi, X. Feng, *Polym. Chem.* **2016**, *7*, 4176 – 4181.
[29] E. Jin, M. Asada, Q. Xu, S. Dalapati, M. A. Addicoat, M. A. Brady, H. Xu, T. Nakamura, T. Heine, Q. Chen, D. Jiang, *Science* **2017**, *357*, 673 – 676.
[30] S. Bi, C. Yang, W. Zhang, J. Xu, L. Liu, D. Wu, X. Wang, Y. Han, Q. Liang, F. Zhang, *Nat. Commun.* **2019**, *10*, 2467.
[31] D. Schwarz, Y. Noda, J. Klouda, K. Schwarzová-Pecková, J. Tarábek, J. Rybáček, J. Janoušek, F. Simon, M. V. Opanasenko, J. Čejka, A. Acharjya, J. Schmidt, S. Selve, V. Reiter-Scherer, N. Severin, J. P. Rabe, P. Ecorchard, J. He, M. Polozij, P. Nachtigall, M. J. Bojdys, *Adv. Mater.* **2017**, *29*, 1703399.
[32] J. Guo, Y. Xu, S. Jin, L. Chen, T. Kaji, Y. Honsho, M. A. Addicoat, J. Kim, A. Saeki, H. Ihee, S. Seki, S. Irle, M. Hiramoto, J. Gao, D. Jiang, *Nat. Commun.* **2013**, *4*, 2736.
[33] Z. Meng, R. M. Stolz, K. A. Mirica, *J. Am. Chem. Soc.* **2019**, *141*, 11929 – 11937.
[34] X. Li, H. Wang, H. Chen, Q. Zheng, Q. Zhang, H. Mao, Y. Liu, S. Cai, B. Sun, C. Dun, M. P. Gordon, H. Zheng, J. A. Reimer, J. J. Urban, J. Ciston, T. Tan, E. M. Chan, J. Zhang, Y. Liu, *Chem* **2020**, *6*, 933 – 944.
[35] J. Kim, A. Elabd, S.-Y. Chung, A. Coskun, J. W. Choi, *Chem. Mater.* **2020**, *32*, 4185 – 4193.
[36] N. A. A. Zwaneveld, R. Pawlak, M. Abel, D. Catalin, D. Gigmes, D. Bertin, L. Porte, *J. Am. Chem. Soc.* **2008**, *130*, 6678 – 6679.
[37] S. Wang, Q. Wang, P. Shao, Y. Han, X. Gao, L. Ma, S. Yuan, X. Ma, J. Zhou, X. Feng, B. Wang, *J. Am. Chem. Soc.* **2017**, *139*, 4258 – 4261.
[38] M. Matsumoto, L. Valentino, G. M. Stiehl, H. B. Balch, A. R. Corcos, F. Wang, D. C. Ralph, B. J. Mariñas, W. R. Dichtel, *Chem* **2018**, *4*, 308 – 317.
[39] A. M. Evans, L. R. Parent, N. C. Flanders, R. P. Bisbey, E. Vitaku, M. S. Kirschner, R. D. Schaller, L. X. Chen, N. C. Gianneschi, W. R. Dichtel, *Science* **2018**, *361*, 52 – 57.
[40] T. Ma, E. A. Kapustin, S. X. Yin, L. Liang, Z. Zhou, J. Niu, L.-H. Li, Y. Wang, J. Su, J. Li, X. Wang, W. D. Wang, W. Wang, J. Sun, O. M. Yaghi, *Science* **2018**, *361*, 48 – 52.
[41] Y. S. Kochergin, Y. Noda, R. Kulkarni, K. Škodáková, J. Tarábek, J. Schmidt, M. J. Bojdys, *Macromolecules* **2019**, *52*, 7696 – 7703.
[42] a) H. Bildirir, V. G. Gregoriou, A. Avgeropoulos, U. Scherf, C. L. Chochos, *Mater. Horiz.* **2017**, *4*, 546 – 556; b) R. S. Sprick, J. X. Jiang, B. Bonillo, S. Ren, T. Ratvijitvech, P. Guiglion, M. A. Zwijnenburg, D. J. Adams, A. I. Cooper, *J. Am. Chem. Soc.* **2015**, *137*, 3265 – 3270; c) B. Bonillo, R. S. Sprick, A. I. Cooper, *Chem. Mater.* **2016**, *28*, 3469 – 3480.
[43] Y. Noda, C. Merschjann, J. Tarábek, P. Amsalem, N. Koch, M. J. Bojdys, *Angew. Chem. Int. Ed.* **2019**, *58*, 9394 – 9398; *Angew. Chem.* **2019**, *131*, 9494 – 9498.
[44] Y. S. Kochergin, D. Schwarz, A. Acharjya, A. Ichangi, R. Kulkarni, P. Eliášová, J. Vacek, J. Schmidt, A. Thomas, M. J. Bojdys, *Angew. Chem. Int. Ed.* **2018**, *57*, 14188 – 14192; *Angew. Chem.* **2018**, *130*, 14384 – 14388.

[45] D. Schwarz, A. Acharjya, A. Ichangi, Y. S. Kochergin, P. Lyu, M. V. Opanasenko, J. Tarábek, J. Vacek Chocholoušová, J. Vacek, J. Schmidt, J. Čejka, P. Nachtigall, A. Thomas, M. J. Bojdys, *ChemSusChem* **2019**, *12*, 194 – 199.
[46] J. Lee, O. Buyukcakir, T. W. Kwon, A. Coskun, *J. Am. Chem. Soc.* **2018**, *140*, 10937 – 10940.
[47] Y. Jiao, Z. Ye, F. Wu, A. Xie, W. Zhao, L. Wu, X. Zhu, W. Dong, *ACS Appl. Nano Mater.* **2020**, *3*, 4553 – 4561.
[48] T. Li, W. Zhu, R. Shen, H.-Y. Wang, W. Chen, S.-J. Hao, Y. Li, Z.-G. Gu, Z. Li, *New J. Chem.* **2018**, *42*, 6247 – 6255.
[49] M. Ratsch, C. Ye, Y. Yang, A. Zhang, A. M. Evans, K. Borjesson, *J. Am. Chem. Soc.* **2020**, *142*, 6548 – 6553.
[50] a) Y. Byun, L. S. Xie, P. Fritz, T. Ashirov, M. Dinca, A. Coskun, *Angew. Chem. Int. Ed.* **2020**, *59*, 15166 – 15170; *Angew. Chem.* **2020**, *132*, 15278 – 15282; b) Y. Byun, A. Coskun, *Angew. Chem. Int. Ed.* **2018**, *57*, 3173 – 3177; *Angew. Chem.* **2018**, *130*, 3227 – 3231.
[51] T. Ben, K. Shi, Y. Cui, C. Pei, Y. Zuo, H. Guo, D. Zhang, J. Xu, F. Deng, Z. Tian, S. Qiu, *J. Mater. Chem.* **2011**, *21*, 18208.
[52] G. Lin, H. Ding, R. Chen, Z. Peng, B. Wang, C. Wang, *J. Am. Chem. Soc.* **2017**, *139*, 8705 – 8709.
[53] H. Li, J. Chang, S. Li, X. Guan, D. Li, C. Li, L. Tang, M. Xue, Y. Yan, V. Valtchev, S. Qiu, Q. Fang, *J. Am. Chem. Soc.* **2019**, *141*, 13324 – 13329.
[54] H. Ding, J. Li, G. Xie, G. Lin, R. Chen, Z. Peng, C. Yang, B. Wang, J. Sun, C. Wang, *Nat. Commun.* **2018**, *9*, 5234.
[55] A. Acharjya, P. Pachfule, J. Roeser, F.-J. Schmitt, A. Thomas, *Angew. Chem. Int. Ed.* **2019**, *58*, 14865 – 14870; *Angew. Chem.* **2019**, *131*, 15007 – 15012.
[56] T. Jadhav, Y. Fang, C. H. Liu, A. Dadvand, E. Hamzehpoor, W. Patterson, A. Jonderian, R. S. Stein, D. F. Perepichka, *J. Am. Chem. Soc.* **2020**, *142*, 8862 – 8870.
[57] Y. Meng, Y. Luo, J. L. Shi, H. Ding, X. Lang, W. Chen, A. Zheng, J. Sun, C. Wang, *Angew. Chem. Int. Ed.* **2020**, *59*, 3624 – 3629; *Angew. Chem.* **2020**, *132*, 3653 – 3658.
[58] a) X. Huang, H. Yao, Y. Cui, W. Hao, J. Zhu, W. Xu, D. Zhu, *ACS Appl. Mater. Interfaces* **2017**, *9*, 40752 – 40759; b) X. Huang, P. Sheng, Z. Tu, F. Zhang, J. Wang, H. Geng, Y. Zou, C. A. Di, Y. Yi, Y. Sun, W. Xu, D. Zhu, *Nat. Commun.* **2015**, *6*, 7408.
[59] Z. Meng, R. M. Stolz, L. Mendecki, K. A. Mirica, *Chem. Rev.* **2019**, *119*, 478 – 598.
[60] B. Nath, W.-H. Li, J.-H. Huang, G.-E. Wang, Z.-h. Fu, M.-S. Yao, G. Xu, *CrystEngComm* **2016**, *18*, 4259 – 4263.
[61] G. Skorupskii, M. Dinca, *J. Am. Chem. Soc.* **2020**, *142*, 6920 – 6924.
[62] T. Chen, J. H. Dou, L. Yang, C. Sun, N. J. Libretto, G. Skorupskii, J. T. Miller, M. Dinca, *J. Am. Chem. Soc.* **2020**, *142*, 12367 – 12373.
[63] A. J. Heeger, *Adv. Mater.* **2014**, *26*, 10 – 27.
[64] R. Gutzler, *Phys. Chem. Chem. Phys.* **2016**, *18*, 29092 – 29100.
[65] T. Banerjee, F. Podjaski, J. Kröger, B. P. Biswal, B. V. Lotsch, *Nat. Rev. Mater.* **2021**, *6,* 168 – 190.
[66] T. H. Le, Y. Kim, H. Yoon, *Polymers* **2017**, *9*, 150.